Heliyon 10 (2024) e34501

Contents lists available at ScienceDirect

Heliyon

journal homepage: www.cell.com/heliyon

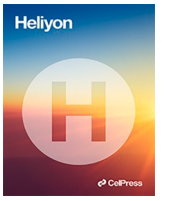

Research article

Calculating toxic pressure for mixtures of endocrine disruptors

Tom M. Nolte [1]

Department of Environmental Science, Institute for Water and Wetland Research, Radboud University Nijmegen, 6500, GL Nijmegen, the Netherlands

A B S T R A C T

Incidence of autoimmune disorders, birth defects, and neurological diseases rose over the past 50 years due to increasing variety and quantity of pollutants. To date, there appear few methods capable to evaluate and predict mixture effects by endocrine disruptors (EDs). For the first time, we have developed calculus to determine mixture effects by all kinds of EDs.

Our method uses the golden ratio ϕ and draws from bifurcation and chaos theory. Using also the concept of molecular mimicry, we developed the equation: $effect = \frac{100\%}{1+e^5 \cdot \sum K_i [C_i]^{-n_i \phi^5}}$. We successfully tested the equation using a range of cohort studies and biomarkers, and for different pollutants like heavy metals, thyroid hormone mimickants, chromate/chlorate, etc.

The equation is simple enough to use with only minor prior knowledge and understanding of basic algebra. The method is universal and calculation is data 'light', requiring only pollutant concentrations [*C*], potencies *K* and an integer *n* for endocrinal involvement. This study offers a comprehensive framework to assess the health effects of pollutant exposure across diverse populations, envisioning far-reaching impact, and presenting practical examples and insights.

1. Introduction

Incidence of autoimmune disorders, birth defects, neurological diseases and even dysregulation of body temperature rose over the past decades in industrialized countries [1–4]. Environmental exposure, rather than genetics, is the most important factor in the observed trends [5]. While disease can appear later in life, decreases in health match rises in pollutant exposures and past peaks thereof [6]. Radically different approaches may reverse the trends, with emphasis on early detection [7]. Toxicity of chemical mixtures is of concern considering the increased variety and quantity of chemicals on the market and environment [8,9]. Children exposed to a pollutant mixture show more malformations, but many factors can obscure associations [10]. It is the mixture, or total body burden of exposure to pollutants, that is relevant. Proving the toxicity of a mixture, however, is like a blind man in a dark room looking for a large, agile, polymorphic, lethal, black cat that certainly is there. Understanding sources, aspects and reasons of mixture toxicity helps to move towards socially responsible use of chemicals to save lives, resources and money [11].

Mixture toxicity is particularly of concern for endocrine disrupting chemicals (EDCs) [9], which exert disruption at infancy with effects throughout lifetime. Metabolism and growth are driven by the endocrine system: in response to the pituitary gland and hypothalamus, the thyroid produces hormones for fetal and childhood growth and central nervous system development. Thyreotropin releasing hormone (TRH) from the hypothalamus stimulates pituitary thyrotropic cells to secrete thyroid stimulating hormone (TSH). This stimulates follicular thyroid cells to synthesize and secrete thyroxin (T_4) and calcitonin. Along with the parathyroid hormone and calcitriol from the kidneys [12], these optimize and control the availability of Ca^{2+}, Mg^{2+}, PO_4, I^- and triiodothyronine (T_3), essential to growth, in blood serum and cytosol. TSH affects these concentrations throughout the fetus or neonate to stay within bandwidths for

E-mail address: tom.m.nolte@gmail.com.

[1] Current address: Naturalis Biodiversity Institute, Darwinweg 2, 2333 CR Leiden, The Netherlands.

https://doi.org/10.1016/j.heliyon.2024.e34501

Received 23 February 2024; Received in revised form 1 July 2024; Accepted 10 July 2024

Available online 11 July 2024

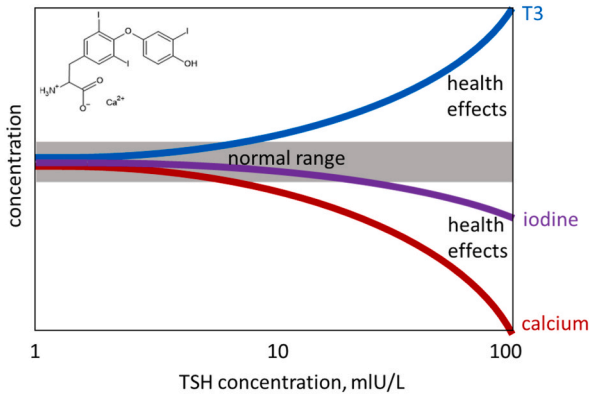

Fig. 1. Schematic representation of changes in thyroid hormone, iodine and calcium (ng/L, not to scale) with increasing severity of illness. Adapted from [17].

'normal' growth, Fig. 1. Thereby, they unlock codes (i.e., DNA) for growth, differentiation, etc. Stressing this unveils regulatory feedback, as TSH and T_3 are positively correlated [13]; iodine and Ca^{2+} are negatively correlated to TSH [14–16], Fig. 1.

The concept of molecular mimicry attracts considerable research related to the genesis of autoimmune disorders and endocrine disease [7]. TH-mimicking pollutants affect structure and function of thyroid [18]. Due to their structure/flexibility, they fit receptors to cloud signals for differentiation. Endocrine disruption is like picking a lock with a deformed or malleable key, hijacking the routes to specialization. Mimickants decrease the 'correct' number of locks opened. In disturbed thyroid homeostasis, the thyroid can be overactive (hyperthyroidism). Mimicking TH distorts balance to increase likelihood of symptoms. To asses mixture toxicity, we sought a common factor within these regulatory mechanisms. To identify pollutants, we need information on normal development during pregnancy and early infancy, and characterization of targets for toxic modes of action (TMoA). The question is, how to evaluate toxicity for a mixture, wherein chemicals operate under seemingly different MoA? In the Supplementary Information (SI) of this paper, we review targets and metabolism for THs, I^- and Ca^{2+} and their disfunctioning as result of EDCs and relationship to TSH. This introduction continues with Section 1.1.

1.1. TSH as a dose metric for mixtures

Decades of research aimed at finding suitable dose metrics for mixtures. 'Concentration addition' and 'independent action' claim to predict mixture toxicity for EDCs [19,20]. We may not 'add' toxicities across different mechanisms because chemicals bind preferentially to different receptors, have different molecular initiating events and interfere with signaling pathways in different ways: 1) EDCs that block Ca-channels lower target calcium. 2) EDCs that block I-channels lower target iodine. 3) EDCs that block TH receptors lower target T_3. All EDC types increase TSH as metabolic pathways merge at TSH, their common factor. TSH, as a biomarker, may capture their combined effects for a mixture of EDC types. Blockings of Ca/I/TH are all associated with higher TSH, via $[T_4] \propto 1/[T_{3mimickant}]$ and $[I^-] \propto 1/[I_{mimickant}]$ and $[Ca^{2+}] \propto 1/[Ca^{2+}_{mimickant}]$, see Fig. 2. Chronic hypersecretion of TSH in neonates then relates to numerous health-issues, decrease in memory, cognitive and executive function [21–23].

The human body is self-repairing; the more damage there is, the more repair the body needs (*repair∝damage*): 'stress prompts TSH to remediate problems'. Repair differs for pollutants, e.g., glutathione for heavy metals vs. arylhydrocarbon receptor (AHR) for dioxins, having different capacities, sensitivities and thresholds. The more repair the body needs, the more TSH it produces (*TSH→repair*). By analogy, the body may 'sense' high calcium in blood, due to Ca^{2+} mimickants, and tries to reduce it by producing calcitonin. TSH alters I^-_{intr}, T_4 and calcium levels to push back against imbalance, towards natural balance, so to unobstruct growth and differentiation. TSH alters Ca/T_4 to eliminate heavy metals and T_3-mimickants in favor of trace metals and T_3. We combine toxicities (red) by looking at repair (green) in Fig. 2. There is a natural 'unexposed' healthy baseline of TSH, approximately logarithmically distributed among people. As exposure metric, we chose TSH that captures exposure to all EDCs (see Supplementary Information, SI), central to developmental disorders. We define exposure as $(TSH - TSH_{ref})$, with TSH_{ref} the TSH for 'non-exposed' people, 1.3 mIU/L, with 68 % range between 0.8 and 2 mIU/L) [24–27].

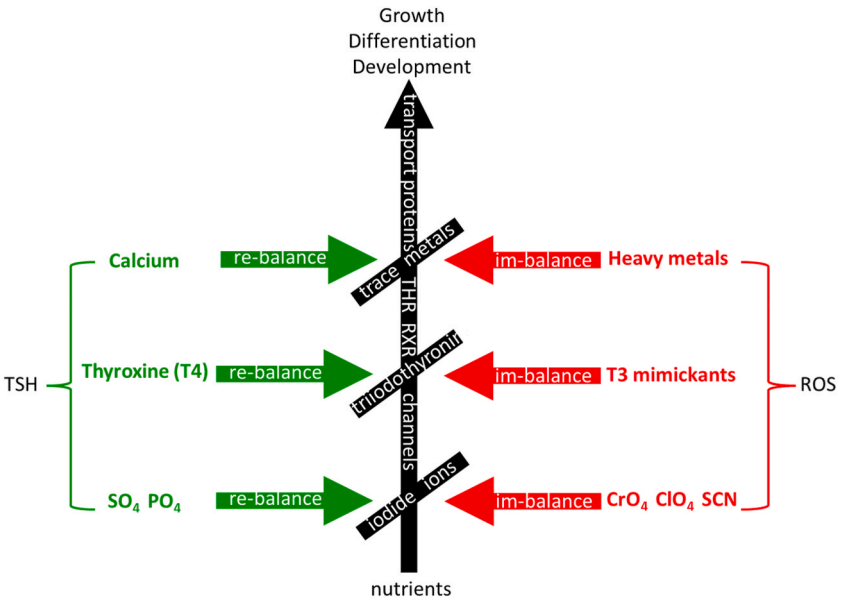

Fig. 2. Depending on levels of endocrine disrupting chemicals (red), the human body needs to allocate hormones and cations/anions (green) to ensure that nutrients remain incorporable via metabolic schemes for growth. (For interpretation of the references to colour in this figure legend, the reader is referred to the Web version of this article.)

2. Methods

2.1. Calculating TSH levels

Repair of damage proceeds via TSH. As all heavy metals mimic Ca^{2+}, Zn^{2+}, etc. their effects on TSH stack. As all T_3 mimickants mimic T_3, their effects on TSH also stack. As Ca^{2+}, T_3 and iodine are interrelated via TSH, the effects of their mimicking EDCs analogs also stack, to increase TSH. Considering stoichiometry, we can add the terms (potent concentrations in blood plasma) for mimickants (M)[2], Eq. (1):

$$TSH - TSH_{ref} = \left(\sum_{1}^{IM}\frac{[C_{IM}]_{plasma}}{K_{IM}}\right)^{\frac{\phi^2}{4}} + \left(\sum_{1}^{T3M}\frac{[C_{T3M}]_{plasma}}{K_{T3M}}\right)^{\frac{\phi^2}{1}} + \left(\sum_{1}^{CaM}\frac{[C_{CaM}]_{plasma}}{K_{CaM}}\right)^{\frac{\phi^2}{1}} \quad (1)$$

Summations (Σ) within compound classes within the same MoA are common practice in RA (e.g., 'total equivalents' TEQ [28]). Dioxin-like mixtures decrease T_4 levels additively [22]. Adding effects on TSH in Eq. (1) is equivalent to using e.g., equivalency factors or the 'Toxic Unit' approach[3], but measures both toxicity *and* repair, the amount of repair needed. We used potencies *K*, benchmarked in Section 2.2-2.4. ϕ is a growth factor. Depending on dose, T_3 and Ca^{2+} mimickants have either synergetic or antagonistic effects [29], acting at the same or different binding sites. A golden ratio ϕ in concentration distinguishes between binding modes when adding effects [30] (more info on ϕ in Section 3.2).

The number 2 in ϕ^2 represents connectivity [31–33]: 2 sites for T_3(M) per TR [34]; 2 sites in metal-binding proteins [35]; 2 DNA spirals wind around 2 copies of histones; 2 S-adenosyl-L-homocysteine cofactors bind at 2 CpG sites of the methyltransferase dimer to inhibit 2 consecutive steps of DNA methylation [36,37]. The 4 (in Eq. (1)) is the number of I atoms associated with blocking a receptor or channel. For 1 T_3 molecule interacting with a TR, 4 I atoms need to be blocked to effectuate the same sized response as that of T_3 (and Ca^{2+}) antagonists. We substantiated the exponents with data in Figs. 3–6: $\phi^2 = 2.6$, and the ratio of exponents (2.6/0.6) gives 4, i.e., the ('stoichiometric') number of I-atoms to synthesize T_4. As T_3Ms have similar MoA (mimicking T_3), we take identical exponents in each T_3M-TSH response relationship.

[2] Technically, CaM and T_3M may be 'umbrella-d' within the same summation due to their similar exponent, which is reflected by e.g., them binding (MIDAS in) integrins with same stoichiometry. In this respect, the amount of heavy metals determines the amount of binding sites, and the amount of T_3M determines the amount of binding.

[3] $TU = C_1/EC50_1 + C_2/EC50_2 + C_3/EC50_3 + \text{etc.}$

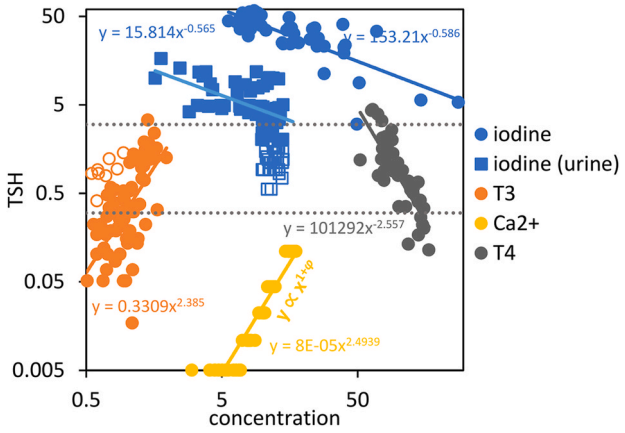

Fig. 3. Calcium, iodine and T_3/T_4 versus TSH. Dotted grey lines are the 95 % ranges for normal TSH levels: in this range, negative feedback establishes healthy homeostasis (open symbols). Data from Yagi (T_4) [38], Karaoglan (iodine) [39], Hamza (urinary iodine) [40], Levine (calcium) [15], and Wang (T_3) [13]. Other data corroborates the exponent for T_3, 2.6 ± 0.5 [41].

2.2. Potencies K for heavy metals

T_3-TR binding is affected by M (Ca^{2+}, Zn^{2+}, etc.) antagonists. Methionine, cysteine, etc. are conserved residues among various TH and nuclear receptors. Therefore, toxic MoAs are similar among heavy metals. Combined bio-concentrations of different metals determines toxicity [49–51]. Heavy metals differ in toxic potency due to receptor binding, bioavailability and signaling type(s). For example, Pb^{2+} binds calmodulin stronger than does Ca^{2+} [52]. There is a ~20 factor higher proportion of methylmercury over mercury in blood as compared to methyl lead over lead [53]. We benchmark K_{CaM} values on Pb using dose-effect data, and calculate K_{CaM} by Eq. (2).,

$$K_{CaM} = 10^{log\ K_{Pb} - (log\ EC_{50,Pb} - log\ EC_{50,CaM})} \quad (2)$$

with K_{Pb} = 100.000 ng/L (Fig. 4), and EC50 data from Ref. [54], indicative for growth inhibition and endocrine disruption [50]. For example, $10^{(logEC50,Pb - logEC50,Hg)} = 20$ [53,54]. Values for TSH and heavy metal concentrations in blood from the open literature substantiate the relative potencies K: offsets between power laws, Fig. 4.

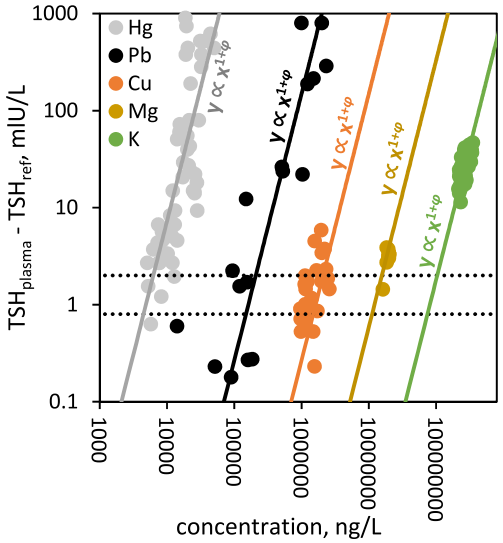

Fig. 4. Concentrations of metals versus TSH-TSH_{ref}. Offset between each relationship (solid lines) indicates potency K. TSH_{ref} = 1.2 mIU/L.

2.3. Potencies K for T_3 mimickants

K thus characterizes potency. We obtained *K* for T_3Ms that block TRs by considering that the extent of binding is determined by properties of the pollutant: binding in the TR and the bioavailability. We express binding, as relative to T_3, by a free-energy relationship [55,56] (Fig. 5A) and thermochemical calculation [57][4]:

$$K_{T3M} = 10^{log\ K_{T3} - \left(2 \cdot 2.3 \cdot \left[\left(E_{HOMO,T3M} - E_{HOMO,T3}\right) + RT\left(pK_{a,T3M} - pK_{a,T3}\right)\right]\right) - \left(log\ K_{OW,T3M} - log\ K_{OW,T3}\right)} \quad (3)$$

with K_{T3} the plasma concentration of T_3 at 1 mIU/L TSH (1000 ng/L, Fig. 5B), and $\log K_{OW,T3} = 0.9$ [58]. The number of binding places within the TR is 2 [34]. Histidines are conserved residues among TH and nuclear receptors. Binding takes place by proton and electron exchange between histidine and tyrosine [34,59–63], with a possible halogen-sulfur bond [64]. We obtain receptor binding values via the energy of the highest occupied molecular orbital (E_{HOMO}) of T_3M, where $E_{HOMO,T3}$ -9.0 eV on the tyrosyl phenol OH ($pK_{a,T3} = 8$). Values for e.g. TCDD, $\log K_{OW} = 6.8$ [65] and $E_{HOMO,T3M} = -9.3$ eV[5] yield 2•2.3•(-9.3 + 9.0) = −1.2. Then, $\log K_{T3M} = -1.2\text{-}(0.9\text{–}6.8) = 4.6$. Thus, TCDD is $10^{4.6}$ times more potent than T_3, substantiated by literature: TCDD induces AhR at $\sim 10^{-12}$ M [66] and T_3 at $\sim 10^{-8}$ M [67]. Fig. 5B substantiates Eq (3): $10^{\sim 4\text{-}5}$ times higher *K* of TCDD than T_3.

2.4. Potencies K for iodine mimickants

The sodium/iodide symporter (NIS) concentrates anions in the thyroid. Histidine, etc. are conserved residues in NIS transporters. 'Ate' anions differ in toxic potency due to affinity (∼EC) with the NIS. Affinity of ClO_4 is 10-fold and ∼200-fold higher than for I^- and ClO_3 [42], resp [42,68]. At pH∼7, there is a ∼10.000 factor higher proportion of AsO_4 over total As in blood (pH∼7.5) as compared to CrO_4 over total Cr [69]. We benchmark K_{IM} values on AsO_4 which has dose-effect data. We neglect methylation of As, and calculate:

$$K_{IM} = 10^{log\ K_{AsO_4} - \left(log\ EC_{50,AsO_4} - log\ EC_{50,IM}\right) - \left(\log \frac{[AsO_4]}{[total\ As]} - \log \frac{[IM]}{[totalM]}\right)} \quad (4)$$

with $K_{AsO4} = 10.000$ ng/L. Data on relative potencies of NIS inhibitors from Refs. [68,70]. Affinities for SCN^- and I^- for the NIS transporter are similar; both 10-fold less than ClO_4 [42,68,71]. SCN^- is a redox-active growth regulator [72]: MPO or TPO/H_2O_2 [73] oxidizes SCN^- (subsequently) into $OSCN^-$ [74,75], OCN [76] and CN^- [77,78]. SCN^- toxicity is effectuated via CN^- [74,79]; we take the ratio of SCN^- over CN^- in blood as 200 [80], i.e., $10^{[\log(CN/SCN)]} = 0.005$. In turn we take $10^{-(logEC50,AsO4\text{-}logEC50,SCN)} = 10$, because of 10-fold higher NIS-affinity [42,68]. As high oxidation potential in the thyroid converts Cr^{3+} to CrO_4 [81,82], we take $10^{-(logEC50,\ AsO4\text{-}logEC50,CrO4)} = 10.000$, matching concentration ratios [69]. In turn we take $10^{-[\log(AsO4/totalAs)\ -\ \log(Cr3+/totalCr)]} = 1$. Offsets between relationships in Fig. 6, substantiate *K* values.

2.5. Exposure metric risk metric

The concept of 'exposure' only makes sense if we benchmark it against an effect, the result of exposure. In Eq. (5), the exponent is a growth factor, putting the risk of damage (via 'excess' TSH) in context of normal growth across conditions and factors. We presume it be ϕ (see discussion for details):

$$risk = \left(TSH - TSH_{ref}\right)^{\phi} \quad (5)$$

To obtain the exponent (ϕ?), we compared risk with human health effect data. We use a logit equation to compare probabilities of human health being affected with our exposure metric:

$$ln\left(\frac{p}{1-p}\right) = \phi \cdot ln\left(TSH - TSH_{ref}\right) - c \quad (6)$$

where *p* is probability: $p = \frac{effect\%}{100\%}$. *c* is a mathematical and biochemical constant extractable from regression.

To perform regression, we collected health endpoints (TSH-health response data) from both human cohort, and biomarker studies with endpoints of varying complexity. We applied 10 in vitro biomarkers and 20 different human cohort studies. We pooled the data for different health effects on brain, kidney, bone, heart, etc. In other words, we did not distinguish between different effects: as long as they represent an average human or population (data in SI). We obtained *p* values via Eq. (7):

$$p = \left(\frac{effect - effect_{min}}{effect_{max} - effect_{min}}\right) \quad (7)$$

wherein the $effect_{min}$ corresponds to TSH = 1.2 mIU/L for 'healthy' (control) subjects in case of cohort studies. 1.2 mlU/L corresponds to the background incidence of health effects [1–4] presumably in absence of pollutants (i.e., the 'unexposed' case). TSH_{ref} values for

[4] size exclusion is not incorporated in the calculation of potency of pollutants (Eq. (3)), thus valid for small EDCs.
[5] here $RT(pK_{a,T3M}\text{-}pK_{a,T3}) = 0$ as TCDD has no tyrosyl-OH.

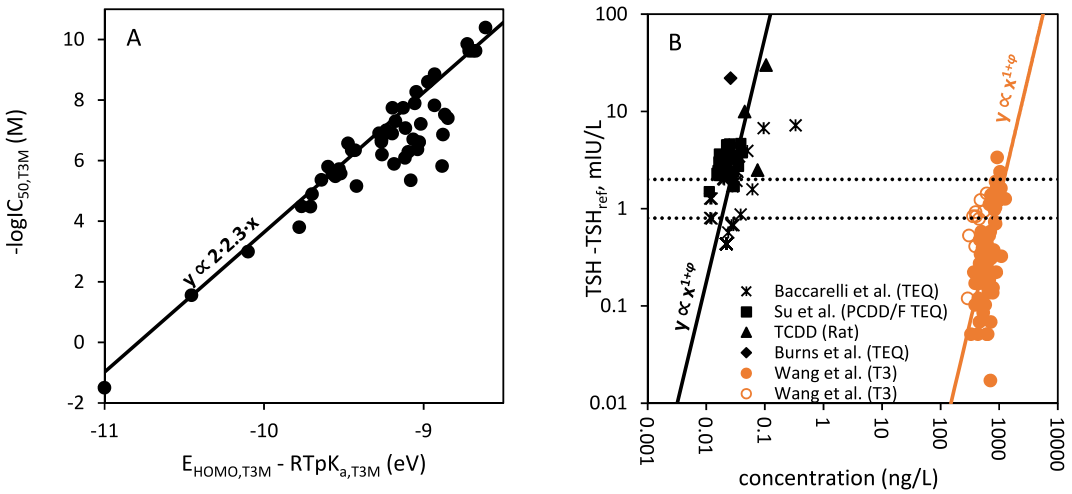

Fig. 5. Fig. 5A. Induction concentration values for the thyroid hormone receptor α versus indicators of electron and proton transfer energies, E_{HOMO} and pK_a. Outliers are due to missing info on pK_a or bioavailability. Data selection from Ref. [42].
Fig. 5B. Effect on TSH versus concentration dose for dioxins PCBs etc. (TEQ) and T_3. Offsets between the compounds are differences in potency *K*. TSH_{ref} = 1.2 mIU/L (dioxin like substances) and TSH_{ref} = 0.0 mIU/L for T_3.

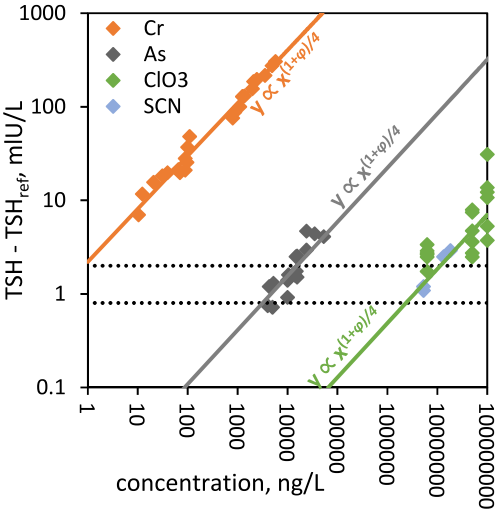

Fig. 6. Concentrations of iodine mimickants versus TSH-TSH_{ref}. Offset between each relationship (solid lines) indicates potency *K*. With TSH_{ref} = 1.2 mIU/L. Data from Hasan [43] and Ahmed [44] (Cr), Molin [45] (As), Hooth [46] (ClO_3), and Banerjee [47,48].

non-healthy subjects, and values for $effect_{max}$ and $effect_{min}$ are the maximum and minimum values for the health status as based on physiological constraints.

3. Results and discussion

3.1. Pollutants-TSH relationships

Using potencies *K*, we derived dose-response relationships between classes of EDCs and TSH. Fig. 7 depicts results from Equations (2)–(4), showing separate relationships for THMs (black), heavy metals (i.e., Ca and trace metal mimickants, blue), and iodide mimickants (green). The difference in both offset and slope of relationships (Fig. 7) clearly captures the different TMoA among pollutant types. The values represent the toxic equivalency to dioxins (total TEQ, in black), Hg (in blue), and arsenic (AsO_4, in green) equivalents. The difference in exponent is visible: ϕ compared to $\phi/4$. Also, the difference in toxic potencies between classes of EDCs clearly differ. ~20 pg/L is the dioxin TEQ concentration corresponding to 1 mIU/L extra TSH (i.e., TSH-TSH_{ref}). In terms of T_3 concentration, 1 mIU/L extra TSH gives 1000 ng/L T_3; to this the results were benchmarked. Should TH (T_3) values be disrupted, the

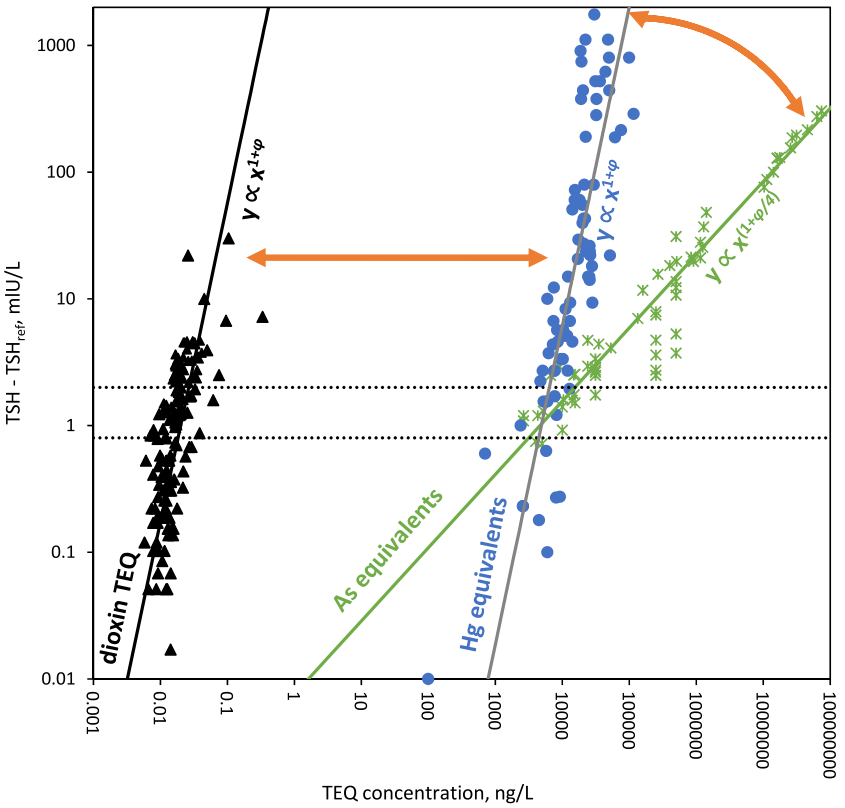

Fig. 7. Concentration of toxicants versus TSH. Sum of all dioxin TEQ (black), in terms of arsenic (green), and in terms of lead (blue). (For interpretation of the references to colour in this figure legend, the reader is referred to the Web version of this article.)

(black) relationship in Fig. 7 provides a risk assessment. This highlights the flexibility of our approach: assessment via T_3, instead of TSH. 1–10 μg/L Hg and As equivalents causes 1 mIU/L extra TSH, Fig. 7.

The potency of Hg and As equivalents is 10^{5-6} times lower than dioxin TEQ, Fig. 7. Lipophilicity (i.e., K_{OW}) of e.g., methylmercury is concomitantly 10^6 times lower than the dioxin TCDD. Also, the concentration in plasma of T_3 (~2 nmol/L) is 10^6 times lower than Ca (~2 mmol/L), reflecting degrees of their metabolic involvement. Both lipophilicity and metabolic involvement explain the offset between relationships, Fig. 7. Assuming the 3 relationships represent their respective chemical groups: contemporary 'safe' or 'normal', 'exposed' (background) values of 5.8 μg/L MeHg [83,84], 10 pg/g lipid (~20 pg/L) dioxin (TEQ) [85,86] and ~1 μg/L arsenic [87] in blood, would give (TSH-TSH$_{ref}$) values of 2 mIU/L, 1 mIU/L, and 0.5 mIU/L. Taken together, an individual would have a (TSH-TSH$_{ref}$) value of 3.5 mIU/L and, hence, TSH = 4.7 mIU/L. The uncertainty associated with this value means it cannot be distinguished from the traditionally accepted upper limit of 4.5 mIU/L [88]. Data in Fig. 7 come from cohort studies and likely entail a degree of co-exposure, though relationships are obvious and, hence, convolution of the parametrization from co-exposures is limited. Fig. 7 is a reflection of specialist studies, e.g., gold miners handling mercury, Italians in vicinity of the Seveso chemical factory (dioxin release), and people with high (shell)fish diet polluted with arsenic [45].

The combined setups of the studies (higher 'signal to noise'?) permitted visualizing the relationships in Fig. 7, whereas with more convoluting factors, i.e. (undocumented) co-exposures, but also nutrition/lifestyle/age etc., would have rendered relationships (Fig. 7) less obvious [89,90]. Many other studies report marginal significance of TSH/pollutant relationships [91]. Uncertainty associated with the relationships (2SD) is approx. a factor 10; this matches the uncertainty factor of 10 for intra-human pharmacokinetic- and dynamic variability [92]. The variance ('cloudiness of points') is not likely due to incomplete data on pollutants within chemicals class (i.e MoA) as a limited number of chemicals are well representative of the entire class [93]. The relationships are a theoretical representation of the body's response given near-infinite resources, but in real-life situation, TSH production may be hampered by biochemical and physiological constraints. Victor Yushchenko, for example, was exposed to 108 ng/g TCDD [94], but we cannot presume his TSH was >10.000 mIU/L. Therefore, the relationships indeed represent non-saturated conditions for chronic exposure for growth, differentiation etc. They do not represent acute effects per se. Many studies report chronic to acute-extrapolation, though [95].

3.2. Relationship between TSH and health effects

Using the data on biomarkers we performed a logit regression, to obtain regression coefficients. Across a population of diverse people and TSH>1.2mIU/L we obtained regression constants of $\phi = 1.6$ and $c = 5$, Eq. (6). By comparison to experimental data,

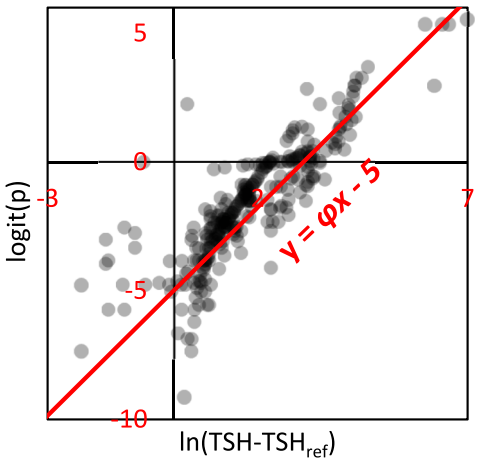

Fig. 8. Relationship between logit p and TSH, wherein logit $p = \ln(p/(1\text{-}p))$, with p as probability.

regression showed ϕ to be (approximated by) the golden ratio ϕ, Fig. 8. From this, we obtained can describe effects based on TSH values, via Eq. (6), alternatively formulated:

$$\%effect = \frac{100\%}{1 + e^{5} \cdot \left(TSH - TSH_{ref}\right)^{-\phi}} \tag{8}$$

ϕ is ubiquitously important in different stages of (human) growth [96–98], regeneration [99,100], development [101–103] and learning [104–107]. Molecular interactions govern optimal development; ϕ represents the mathematical basis for development to achieve ideal form and function. Deregulation of this patterning law may manifest as variation in structure away from that as would be determined by the golden ratio [108]. The golden ratio represents an ideal scenario for growth. We note that exponents in Eq. (1) and Eq. (8) differ: ϕ in the former ϕ^2 in the latter. ϕ and ϕ^2 may distinguish between abnormal (aggravated state) and normal (rest) functioning [32,109,110]. Five-folds are ubiquitous in nature: 5 represents how information from the irrational number ϕ carries over to real-world practice [98,111,112]., The biochemical test for TSH at the heart of this, while different TSH tests exist [113].

If we presume that extrapolation from the regression is possible, we can see that effects at low exposures (ln(TSH-TSH$_{ref}$) are possible, low as they might be. There indeed appears no safe level for dioxins and lead; without safe limits, NOEL or LOEL ought not be used [114]. Effects are minimal at TSH~1.2 mIU/L [115], i.e., are 'purely' due to genetics, nutrition, etc. When TSH-TSH$_{ref}$→0, % effect→0 %, and we return to a 'background' incidence of health effect incidence [1–4]. We can use the TSH level (characterizing same MoAs), to calculate the fraction of the population affected. If, into Eq. (8), we plug in the (Fibonacci) numbers TSH = 21 mIU/L and 144 mIU/L, we get ~50 % and ~95 % effect. One may regard these as 'effect concentrations' EC_{50} and EC_{95} for TSH. Premature death is equivalent to 100 % as all bodily functions shut down. In programmed cell death, all cellular functions shut down.

We compared the relationship between TSH and effect between biomarkers and cohort studies. Fig. 9 shows relationships between elevated TSH (x) and health effects (y), as obtained from human cohort studies (A) and biomarker studies (B). Dose-response curves (Fig. 9A; Fig. 9B) did not significantly differ from each another, with no difference in ϕ between health effects (Fig. 9). Dose-response curves did not statistically differ, apart from a larger spread around the values as expected from Eq. (8). The 'cloudiness of points' in Fig. 9A can be attributed to metadata: compared to bioassays, determining health effects among human cohorts is subject to more confounding factors: nutrition, lifestyle, age, genetics, underlying health effects, unknown exposure to additional endocrine disrupting pollutants, combination effects, etc. We may apply 5 and ϕ as constants for human populations as well. One might argue that exponents *should* differ between health effects because of e.g., expression levels or genetic susceptibility, but ϕ conveniently also describes these factors (spacing and spiraling of DNA, amino acid chains, etc.). Across a population with sufficient diversity, we find no evidence of different exponents ('growth factors') ϕ governing health effects, and values ϕ and 5 would not differ: identicalness represents identical MoA or molecular initiating events.

We can plug TSH levels into Eq. (8), to calculate the fraction of a population effected. The fraction is equivalent to the chance of the individual developing the health effects under chronic exposure. The classic 'upper limit' of TSH of 4.5 mIU/L [88] gives (TSH – TSH$_{ref}$) = 3.3 mIU/L. Using Eq. (8), this value implies an effect of 4 %, or 4 % of people affected. This value is similar to contemporary incidence of congenital diseases such as cryptorchidism [4,6], allergies [116,117], dyslexia [118] and DALY's of the like [119]. Science usually uses a certainty cutoff of 2σ [120], meaning 95 % certainty. A scientific method may thus deem a population 'safe' if 95 % safety is predicted or determined, while 5 % are, in fact, affected. This compares with the 4 %. If for a population a different (e.g., higher) benchmarked TSH$_{ref}$ applies, an effect (%) can still be calculated but the result (% effect) needs also be benchmarked against a potential different (higher) 'background' incidence of health effects.

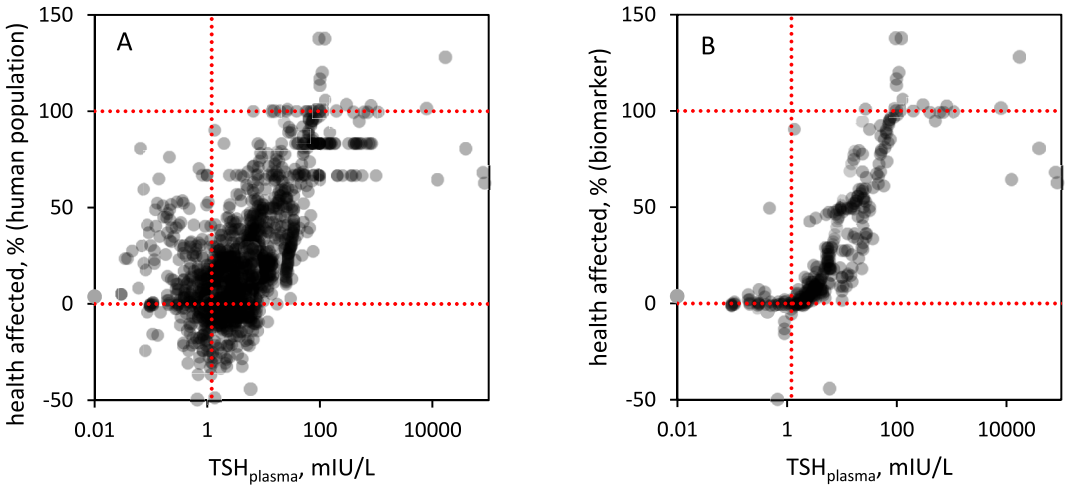

Fig. 9. Relationships between TSH and 20 different health effects (A) and 10 different biomarkers (B), related to Ca^{2+} metabolism, brain, bone, heart, kidney, etc. The red dashed lines are guides to the eye denoting no effect (0 %) and full effect (100 %) and the baseline TSH of 1.2 mUI/L. Spread is larger in A because we are dealing with humans instead of cells, and humans differ in terms of nutrition, lifestyle, etc. (For interpretation of the references to colour in this figure legend, the reader is referred to the Web version of this article.)

4. Outlook

We implemented toxic potencies (K) into Eq (1). Then, from calculations with Eq. (6) emerged 5 and ϕ as constants. K and ϕ in Eq. (1) and Eq. (8) are equivalents of (analogous to) EC_{50} and β in dose-response curves for (eco)toxicity assessments, respectively [50,121]. In conventional (eco)tox modeling and assessment, EC_{50} and β are often 'floating' regression parameters to fit the observed response. β (statistically) represents variability within or among population(s), with respect to MoA and sensitivities [122]. Difference between β for sensitivity distributions are often borderline statistically significant [122]. For a population with sufficient diversity or variability, β values do not differ. Studies claim β to represent MoAs in some way [121,122]. The MoA is an effect pathway due to causal (bio)chemical changes. ϕ does not represent the MoA, rather, it *is* the MoA: the mode by which things (endocrinologically) grow. Unity represents a similar MoA. Therefore, Eq. (1) applies distinct integers (1, 1 and 4) to capture metabolic and stoichiometric involvement (Fig. 7). The exponent can apparently differ according to genetics, nutrition, etc., though, ϕ recurs in multiple underlying parametrizations (Eqs. (1) and (8)). Distinction between MoA and underlying initiating events (IEs) is down to definitions and causality, in a long chain of events. Future work may further compare mixture assessment models capturing different phenomena [30,123,124] similar to Klykov [125], but pending more data [20,126].

β and EC_{50} simultaneously capture factors like population-specific genetics, modulation of metabolic pathways for repair, adaptation to (low) toxic stress [127], DNA methylation and (epigenetic) expression, and competitive binding/crowding at high toxic pressures. Thus, additional biomarkers might aid optimizing results: TSH (cor)relates with lipid profiles [128], prolactin [129], thyroglobulin [130], hemoglobin [131], phosphatase [132], osteopontin [133], peroxidase antibodies, and bone mineral density [134]; in turn relate to inflammation and asthma [135]. Interrelationships (Figs. 3–7) highlight that metabolic pathways are, so some degree, connected as TSH plays a central role in energy metabolism. Infants show negligible difference in TSH between girls or boys. Indeed, cohorts (SI) show that Eq. (1) and Eq. (8) apply to both sexes, though diagnoses differ as (sexual) organs are involved (SI). Pending more data, future work may apply effects on a broader class of TR, RXR and integrins [42,136–140], other cells and receptors, like AhR in lymphocytes [141], peroxysome proliferator activated- and estrogen receptors [142] and transthyretin (TTR) [143] in liver cells, androgen receptors, folate receptor α [144]. For all receptors, models ought to capture mimickants to their respective ligands. Our method aids evaluating cohort studies on the relevance and contribution of ('emerging') pollutants with conflicting results, like ClO_4 [145–147], PFAS/PFOS [148] as relative to total exposure.

Eq. (8) allows customization: one can plug in a new baseline TSH_{ref}, should that deviate from 1.2 mIU/L. Apart from pollutant exposures, multiple factors contribute to thyroid functioning, which may aid optimizing our model to refine prediction for specific cases, groups and cohorts. Left undocumented, variance in stress level, diet, etc. creates uncertainty in thyroid levels, hence model outcome. Age, temperature [149–151], diurnal variations, daily (working [152]) routine like food intake can affect pH [153,154] and (hence) TH levels [155] in blood. To further assess links between pollutant exposure and health, research needs to acknowledge exposure regimes and duration to health effects. Listing β exponents for *all* disease-TSH relationships, plus uncertainties associated, is beyond the scope of this study. The longer the cause-effect-chain, the higher the EC_{50} because, along the way, repair mechanisms intervene to prevent disease onset. The shorter the path towards 'disease', the lower the EC_{50}. The more (stoichiometric) factors (e.g., I atoms) in play, the lower the exponent (Eq. (1)). After infancy disease, a child can outgrow symptoms, provided proper nutrition. Nutrient-dependent potencies ('K', Eq. (1)) may be useful, e.g., mercury/selenium ratios, both as methylating agents [156,157] (SI). This involves interplay between both nutrient-like *and* toxicant-like properties (e.g., cobalt, nitrate).

ϕ captures (effects along) the pathway of cause, exposure and health effect. As ϕ captures initiating events (IEs, Fig. 7) and MoAs (Fig. 8), one may wonder whether not entire cause-effect chains can be described as such. While effect percentages are mathematically rational, mechanisms may appear irrational. Transforming dose to exposure ($\sim C^{\phi^2}$, $\sim TSH^{\phi}$) can be done with complex numbers, $5=(2\phi+e^{i\bullet\pi})^2$, Eq. (8). Probability is not perceptible and suits epidemiological studies: seemingly random effects among similarly exposed individuals. Eq. (8) may capture time as plugging in a benchmarked '1′ yields approximately the Feigenbaum constant [158], describing 'bifurcations' (divisions by cells, divergence of evolutionary species) generically [99,159]. Via ϕ and divergence, Eq. (8) is tied to concepts like spacetime, entropy and chaos theory [160–163]. Bodily disregulation increases with age, as the human body evolves to a state of higher disorder. Chronic versus acute exposure differ in time, but as long as one keeps track how much pollutant is going where (e.g., PBPK and toxicokinetic models [164,165]), both fit within the calculus. Metabolism slows down at higher age, decreasing clearance of pollutants. Both bodily pollutants and TSH in generally increase with age [166], which matches our results. Health effects are indeed more likely later in life, e.g., fertility decrease and memory loss [5,21]. Pollutants and aging affect biochemical circadian and redox clocks (via methylation, phosphorylation, etc.), hence, virtually all metabolic processes [167–170]. We therefore recommend assessing health across lifetime dynamically. Slowing the toxicological clock involves reducing exposure to safeguard human health from mixtures.

Funding

The research that led to this work has not received funding from any source and was a bona fide, self-paid project.

Data availability statement

Further data to reproduce the findings will be shared upon request.

CRediT authorship contribution statement

Tom M. Nolte: Writing – review & editing, Writing – original draft, Visualization, Validation, Resources, Project administration, Methodology, Investigation, Formal analysis, Data curation, Conceptualization.

Declaration of competing interest

The author declares that he has no known competing financial interests or personal relationships that could have appeared to influence the work reported in this paper.

Acknowledgements

I would like to thank Janna Koppe, Gavin ten Tuscher, Marieke Leijs and Paola Movalli for interesting discussion.

Appendix A. Supplementary data

Supplementary data to this article can be found online at https://doi.org/10.1016/j.heliyon.2024.e34501.

References

[1] J.F. Bach, Mechanisms of disease: the effect of infections on susceptibility to autoimmune and allergic diseases, N. Engl. J. Med. 347 (12) (2002) 911–920.
[2] J. Axelsson, et al., Exposure to polychlorinated compounds and cryptorchidism; A nested case-control study, PLoS One 15 (7) (2020) e0236394.
[3] P. Vancamp, B.A. Demeneix, Is the observed decrease in body temperature during industrialization due to thyroid hormone-dependent thermoregulation disruption? Front. Endocrinol. 11 (2020) 470.
[4] EUROCAT. European Surveillance of Congenital Anomalies.https://eu-rd-platform.jrc.ec.europa.eu/eurocat_en.
[5] N.E. Skakkebaek, et al., Male reproductive disorders and fertility trends: influences of environment and genetic susceptibility, Physiol. Rev. 96 (1) (2016) 55–97.
[6] J. Fernandez-Cornejo, et al., Pesticide use peaked in 1981, then trended downward, driven by technological innovations and other factors Statistic: Natural Resources & Environment, USDA Economic Research Service (2014).
[7] D.M. Brady, Autoimmune disease: a modern epidemic? molecular mimicry, the hygiene hypothesis, stealth infections, and other examples of disconnect between medical research and the practice of clinical medicine, Autoimmune Disease. Townsend Letter. 347 (2012) 45–50.
[8] S. Christiansen, et al., Mixtures of endocrine disrupting contaminants modelled on human high end exposures: an exploratory study in rats, Int. J. Androl. 35 (3) (2012) 303–316.
[9] M. Batke, et al., The EU chemicals strategy for sustainability: critical reflections on proposed regulatory changes for endocrine disruptors and mixture toxicity, Arch. Toxicol. 96 (4) (2022) 1133–1135.
[10] J.K. Gurney, et al., Risk factors for cryptorchidism, Nat. Rev. Urol. 14 (9) (2017) 534–548.
[11] K.H. Jones, et al., The other side of the coin: harm due to the non-use of health-related data, Int. J. Med. Inf. 97 (2017) 43–51.
[12] I. Campbell, Thyroid and parathyroid hormones and calcium homeostasis, Anaesth. Intensive Care Med. 12 (10) (2011) 465–468.
[13] W. Wang, et al., Thyroid function abnormalities in COVID-19 patients, Front. Endocrinol. 11 (2020) 623792.

[14] K.A. Heemstra, et al., Thyroid hormone independent associations between serum TSH levels and indicators of bone turnover in cured patients with differentiated thyroid carcinoma, Eur. J. Endocrinol. 159 (1) (2008) 69–76.
[15] B.S. Levine, M. Rodriguez, A.J. Felsenfeld, Serum calcium and bone: effect of PTH, phosphate, vitamin D and uremia, Nefrologia 34 (5) (2014) 658–669.
[16] A. Modi, N. Sahi, Effect of thyroid hormones on serum calcium and phosphorous, Int. J. Clin. Biochem. Res. 5 (4) (2018) 570–573.
[17] J.T. Nicoloff, Abnormal measurements in nonendocrine illness, in: J.W. Hurst (Ed.), Medicine for the Practicing Physician, second ed., Butterworth-Heinemann, 1991.
[18] C.C. Capen, S.L. Martin, The effects of xenobiotics on the structure and function of thyroid follicular and C-cells, Toxicol. Pathol. 17 (2) (1989) 266–293.
[19] N. Hamid, M. Junaid, D.S. Pei, Combined toxicity of endocrine-disrupting chemicals: a review, Ecotoxicol. Environ. Saf. 215 (2021) 112136.
[20] A. Lasch, et al., Mixture effects of chemicals: the difficulty to choose appropriate mathematical models for appropriate conclusions, Environ Pollut 260 (2020) 113953.
[21] C. Freire, et al., Newborn TSH concentration and its association with cognitive development in healthy boys, Eur. J. Endocrinol. 163 (6) (2010) 901–909.
[22] World Health Organization, Endocrine disrupters and child health. Possible Developmental Early Effects of Endocrine Disrupters on Child Health, ISBN9789241503761, 2012.
[23] S.A. Segura, et al., Assessment of thyroid function in the preterm and/or very low birth weight newborn, Anales De Pediatria 95 (4) (2021) 277.e1–277.e8.
[24] M.I. Surks, G. Goswami, G.H. Daniels, The thyrotropin reference range should remain unchanged, Journal of Clinical Endocrinology & Metabolism 90 (9) (2005) 5489–5496.
[25] F. Calaciura, et al., Subclinical hypothyroidism in early childhood: a frequent outcome of transient neonatal hyperthyrotropinemia, J. Clin. Endocrinol. Metab. 87 (7) (2002) 3209–3214.
[26] J. Franklyn, M. Shephard, in: K.R. Feingold, et al. (Eds.), Evaluation of Thyroid Function in Health and Disease, Endotext, South Dartmouth (MA), 2000.
[27] T.E. Hamilton, et al., Thyrotropin levels in a population with no clinical, autoantibody, or ultrasonographic evidence of thyroid disease: implications for the diagnosis of subclinical hypothyroidism, Journal of Clinical Endocrinology & Metabolism 93 (4) (2008) 1224–1230.
[28] E.G.M. Kleijn, E. van der Voet, Dioxines in milieu en voeding in Nederland, Coordinatie-commissie voor de metingen van radioactiviteit en xenobiotische stoffen (1991).
[29] P.M. Hinkle, P.A. Kinsella, K.C. Osterhoudt, Cadmium uptake and toxicity via voltage-sensitive calcium channels, J. Biol. Chem. 262 (34) (1987) 16333–16337.
[30] G.E. Jarvis, A.J. Thompson, A golden approach to ion channel inhibition, Trends Pharmacol. Sci. 34 (9) (2013) 481–488.
[31] J. Prechl, Network organization of antibody interactions in sequence and structure space: the RADARS model, Antibodies 9 (2) (2020) 13.
[32] M.A. Kramer, Golden Rhythms as a Theoretical Framework for Cross-Frequency Organization. Neurons, Behavior, Data Analysis, and Theory, arXiv:2111, 2022 09953.
[33] F. Knox, B. Mohar, D.R. Wood, A Golden ratio inequality for vertex degrees of graphs, Am. Math. Mon. 126 (8) (2019) 742–747.
[34] P.C. Souza, et al., Identification of a new hormone-binding site on the surface of thyroid hormone receptor, Mol. Endocrinol. 28 (4) (2014) 534–545.
[35] C.S. Fullmer, S. Edelstein, R.H. Wasserman, Lead-binding properties of intestinal calcium-binding proteins, J. Biol. Chem. 260 (11) (1985) 6816–6819.
[36] C.C. Lin, et al., Structural insights into CpG-specific DNA methylation by human DNA methyltransferase 3B, Nucleic Acids Res. 17 (48) (2020) 3949–3961.
[37] K. Rai, et al., DNA demethylation in zebrafish involves the coupling of a deaminase, a glycosylase, and gadd45, Cell 135 (7) (2008) 1201–1212.
[38] H. Yagi, et al., Resistance to thyroid hormone caused by two mutant thyroid hormone receptor beta, R243Q and R243W, with marked impairment of function that cannot be explained by altered in vitro 3,5,3'-triiodothyroinine binding affinity, Journal of Clinical Endocrinology & Metabolism 82 (5) (1997) 1608–1614.
[39] M. Karaoglan, E. Isbilen, The role of placental iodine storage in the neonatal thyroid stimulating hormone surge: iodine as a driving force to adapt the terrestrial life, J. Endocrinol. Invest. 44 (5) (2021) 1041–1052.
[40] R. Hamza, et al., Maternal and neonatal iodine nutrition in Cairo, Internet J. Pediatr. Neonatol. 8 (2) (2007) 1–6.
[41] W. Russell, et al., Free triiodothyronine has a distinct circadian rhythm that is delayed but parallels thyrotropin levels, Journal of Clinical Endocrinology & Metabolism 93 (6) (2008) 2300–2306.
[42] N. Li, et al., Study for the binding affinity of thyroid hormone receptors based on machine learning algorithm, SAR QSAR Environ. Res. 33 (8) (2022) 601–620.
[43] H.G. Hasan, T.J. Mahmood, P.A. Ismael, Studies on the relationship between chromium(III) ion and thyroid peroxidase activity in sera of patients with thyroid dysfunction, Ibn Al-Haitham Journal for Pure and Applied sciences 24 (2) (2011).
[44] T.I. Ahmed, S. Irshad, Higher anti-TPO antibody titers are associated with greater thyroid-related symptomatology, European Journal of Molecular and Clinical Medicine 9 (1) (2022) 663.
[45] M. Molin, et al., Arsenic in seafood is associated with increased thyroid-stimulating hormone (TSH) in healthy volunteers - a randomized controlled trial, J. Trace Elem. Med. Biol. 44 (2017) 1–7.
[46] M.J. Hooth, et al., Subchronic sodium chlorate exposure in drinking water results in a concentration-dependent increase in rat thyroid follicular cell hyperplasia, Toxicol. Pathol. 29 (2) (2001) 250–259.
[47] K.K. Banerjee, et al., Effect of thiocyanate ingestion through milk on thyroid hormone homeostasis in women, Br. J. Nutr. 78 (5) (1997) 679–681.
[48] K.K. Banerjee, A. Bishayee, P. Marimuthu, Evaluation of cyanide exposure and its effect on thyroid function of workers in a cable industry, J. Occup. Environ. Med. 39 (3) (1997) 258–260.
[49] X. Xu, et al., Assessment of toxic interactions of heavy metals in multi-component mixtures using sea urchin embryo-larval bioassay, Toxicol. Vitro 25 (1) (2011) 294–300.
[50] T.M. Nolte, et al., Bioconcentration of organotin cations during molting inhibits heterocypris incongruens growth, Environ. Sci. Technol. 54 (22) (2020) 14288–14301.
[51] J.D. Meeker, et al., Multiple metals predict prolactin and thyrotropin (TSH) levels in men, Environ. Res. 109 (7) (2009) 869–873.
[52] M. Kirberger, et al., Metal toxicity and opportunistic binding of Pb(2+) in proteins, J. Inorg. Biochem. 125 (2013) 40–49.
[53] K. Andersson, C.A. Nilsson, O. Nygren, A new method for the analysis of tetramethyllead in blood, Scand. J. Work. Environ. Health 10 (1) (1984) 51–55.
[54] B. Kudlak, L. Wolska, J. Namiesnik, Determination of EC (50) toxicity data of selected heavy metals toward Heterocypris incongruens and their comparison to "direct-contact" and microbiotests, Environ. Monit. Assess. 174 (1–4) (2011) 509–516.
[55] J.D. McKinney, Multifunctional receptor model for dioxin and related compound toxic action: possible thyroid hormone-responsive effector-linked site, Environ. Health Perspect. 82 (1989) 323–336.
[56] Y. Wang, et al., Polarizability and aromaticity index govern AhR-mediated potencies of PAHs: a QSAR with consideration of freely dissolved concentrations, Chemosphere 268 (2021) 129343.
[57] T.M. Nolte, et al., Thermochemical unification of molecular descriptors to predict radical hydrogen abstraction with low computational cost, Phys. Chem. Chem. Phys. 22 (40) (2020) 23215–23225.
[58] C. Hansch, A. Leo, D. Hoekman, Exploring QSAR - Hydrophobic, Electronic, and Steric Constants, American Chemical Society, Washington, DC, 1995, p. 129.
[59] J.J. Hangeland, et al., A new class of high affinity thyromimetics containing a phenyl-naphthylene core, Bioorg Med Chem Lett 15 (20) (2005) 4579–4584.
[60] L. Martinez, et al., Molecular dynamics simulations reveal multiple pathways of ligand dissociation from thyroid hormone receptors, Biophys. J. 89 (3) (2005) 2011–2023.
[61] R.L. Wagner, et al., A structural role for hormone in the thyroid hormone receptor, Nature 378 (6558) (1995) 690–697.
[62] T.A. Zughaibi, I.A. Sheikh, M.A. Beg, Insights into the endocrine disrupting activity of emerging non-phthalate alternate plasticizers against thyroid hormone receptor: a structural perspective, Toxics 10 (5) (2022) 263.
[63] F.F. Wang, et al., Structure-based approach for the study of thyroid hormone receptor binding affinity and subtype selectivity, J. Biomol. Struct. Dyn. 34 (10) (2016) 2251–2267.
[64] R. Wilcken, et al., Addressing methionine in molecular design through directed sulfur-halogen bonds, J. Chem. Theor. Comput. 7 (7) (2011) 2307–2315.

[65] W.Y. Shiu, et al., Physical-chemical properties of chlorinated dibenzo-para-dioxins, Environmental Science & Technology 22 (6) (1988) 651–658.
[66] E.A. Stevens, J.D. Mezrich, C.A. Bradfield, The aryl hydrocarbon receptor: a perspective on potential roles in the immune system, Immunology 127 (3) (2009) 299–311.
[67] R. Vrzal, et al., Activated thyroid hormone receptor modulates dioxin-inducible aryl hydrocarbon receptor-mediated CYP1A1 induction in human hepatocytes but not in human hepatocarcinoma HepG2 cells, Toxicol. Lett. 275 (2017) 77–82.
[68] *Gene name: Solute carrier family member 5 (SLC5A5)*, Solvo Biotechnology. Transporter Book 4th Edition. NIS (Na+/I- Symporter). Aliases: TDH1, Na+/I-Cotransporter, 2018.
[69] A.A. Redha, Removal of heavy metals from aqueous media by biosorption, Arab Journal of Basic and Applied Sciences 27 (1) (2020) 183–193.
[70] B. De Groef, et al., Perchlorate versus other environmental sodium/iodide symporter inhibitors: potential thyroid-related health effects, Eur. J. Endocrinol. 155 (1) (2006) 17–25.
[71] M. Tonacchera, et al., Relative potencies and additivity of perchlorate, thiocyanate, nitrate, and iodide on the inhibition of radioactive iodide uptake by the human sodium iodide symporter, Thyroid 14 (12) (2004) 1012–1019.
[72] J.D. Chandler, B.J. Day, Biochemical mechanisms and therapeutic potential of pseudohalide thiocyanate in human health, Free Radic. Res. 49 (6) (2015) 695–710.
[73] H. Ghorbel, et al., Thiocyanate effects on thyroid function of weaned mice, Comptes Rendus Biol. 331 (4) (2008) 262–271.
[74] USEPA, Toxicological review of hydrogen cyanide and cyanide salts, in: Support of Summary Information on the Integrated Risk Information System (IRIS), EPA/635/R-08/016F, Washington, DC, 2010.
[75] J.D. Chandler, B.J. Day, Thiocyanate: a potentially useful therapeutic agent with host defense and antioxidant properties, Biochem. Pharmacol. 84 (11) (2012) 1381–1387.
[76] C. Delporte, et al., Myeloperoxidase-catalyzed oxidation of cyanide to cyanate: a potential carbamylation route involved in the formation of atherosclerotic plaques? J. Biol. Chem. 293 (17) (2018) 6374–6386.
[77] J. Chung, J.L. Wood, Oxidation of thiocyanate to cyanide catalyzed by hemoglobin, J. Biol. Chem. 246 (3) (1971) 555–560.
[78] J. Chung, J.L. Wood, Oxidation of thiocyanate to cyanide and sulfate by the lactoperoxidase-hydrogen peroxide system, Arch. Biochem. Biophys. 141 (1) (1970) 73–78.
[79] B. Contempre, et al., Thiocyanate induces cell necrosis and fibrosis in selenium- and iodine-deficient rat thyroids: a potential experimental model for myxedematous endemic cretinism in central Africa, Endocrinology 145 (2) (2004) 994–1002.
[80] C.J. Vesey, P.V. Cole, Blood cyanide and thiocyanate concentrations produced by long-term therapy with sodium-nitroprusside, Br. J. Anaesth. 57 (2) (1985) 148–155.
[81] J. Bell, et al., Overlooked role of chromium(V) and chromium(IV) in chromium redox reactions of environmental importance, Acs Es&T Water 2 (6) (2022) 932–942.
[82] T.M. Nolte, et al., Ammonia and chromate interaction explains unresolved Hyalella azteca mortality in Flanders' sediment bioassays, Chemosphere 271 (2020) 129446.
[83] National Research Council (US) Committee on the toxicological effects of methylmercury, Toxicological Effects of Methylmercury, The National Academies Press (US), Washington (DC), 2000.
[84] J.W. Seo, B.G. Kim, Y.S. Hong, The relationship between mercury exposure indices and dietary intake of fish and shellfish in women of childbearing age, Int. J. Environ. Res. Publ. Health 17 (13) (2020) 4907.
[85] EFSA Panel on Contaminants in the Food Chain (CONTAM),, Risk for animal and human health related to the presence of dioxins and dioxin-like PCBs in feed and food, EFSA J. 16 (11) (2018) e05333.
[86] European Commission, Commision Regulation (EC) No 1881/2006 of 19 December 2006 Setting Maximum Levels Certain Contaminants in Foodstuffs, 2006. *L 364 5-L 364, Brussels, 24*.
[87] T.G. Kazi, et al., The correlation of arsenic levels in drinking water with the biological samples of skin disorders, Sci. Total Environ. 407 (3) (2009) 1019–1026.
[88] V. Fatourechi, Upper limit of normal serum thyroid-stimulating hormone: a moving and now an aging target? J. Clin. Endocrinol. Metab. 92 (12) (2007) 4560–4562.
[89] K.L.Y. Christensen, Metals in blood and urine, and thyroid function among adults in the United States 2007-2008, Int. J. Hyg Environ. Health 216 (6) (2013) 624–632.
[90] Y. Park, S.J. Lee, Association of blood heavy metal levels and renal function in Korean adults, Int J Environ Res Public Health 19 (11) (2022) 6646.
[91] M.M. Leijs, et al., Alterations in the programming of energy metabolism in adolescents with background exposure to dioxins, dl-PCBs and PBDEs, PLoS One 12 (9) (2017) e0184006.
[92] D.C. Rice, The US EPA reference dose for methylmercury: sources of uncertainty, Environ. Res. 95 (3) (2004) 406–413.
[93] K. Kitamura, et al., Justification of measurement of eight congeners levels instead of twenty congeners of dioxins for mass screening of human exposure, J. Toxicol. Sci. 26 (3) (2001) 163–168.
[94] O. Sorg, et al., 2,3,7,8-tetrachlorodibenzo-p-dioxin (TCDD) poisoning in Victor Yushchenko: identification and measurement of TCDD metabolites, Lancet 374 (9696) (2009) 1179–1185.
[95] L. Foster, J. Mayer, EPA/600/R-98/152. User guide. Acute to Chronic Estimation U.S. Environmental Protection Agency. Gulf Ecology Division. Gulf Breeze, FL, University of Missouri-Columbia, 1999.
[96] S.P. Paul, Golden spirals and scalp whorls: nature's own design for rapid expansion, PLoS One 11 (9) (2016) e0162026.
[97] W.E. Butler, T.B. Kinane, Ring shape golden ratio multicellular structures are algebraically afforded by asymmetric mitosis and one to one cell adhesion, bioRxiv (2018) 1–11.
[98] M. Loose, et al., Spatial regulators for bacterial cell division self-organize into surface waves in vitro, Science 320 (5877) (2008) 789–792.
[99] M. Lieber, The golden ratio (1.62) as a dimensionless biological constant, South Afr. J. Sci. 112 (9–10) (2016), 2-2.
[100] X.J. Zhang, Z.C. Ou-Yang, Mechanism behind the beauty: the golden ratio appeared in the shape red blood cells, Commun. Comput. Phys. 21 (2) (2017) 559–569.
[101] K. Yalta, S. Ozturk, E. Yetkin, Golden ratio and the heart: a review of divine aesthetics, Int. J. Cardiol. 214 (2016) 107–112.
[102] S. Murali, *Golden Ratio in Human Anatomy*. Project Submitted to the Department of Science and Technology as Part of the Summer Vacation Research Work. DST Inspire Scholar. 171/2009, Department of Mathematics Government College, Chittur Palakkad - 678104, Kerala, India, 2012.
[103] E. Petekkaya, et al., Evaluation of the golden ratio in nasal conchae for surgical anatomy, Ear Nose Throat J. 100 (1) (2021) NP57–NP61.
[104] D. De Bartolo, et al., The role of walking experience in the emergence of gait harmony in typically developing toddlers, Brain Sci. 12 (2) (2022) 155.
[105] M. Iwasaki, Y. Noguchi, R. Kakigi, Two-stage processing of aesthetic information in the human brain revealed by neural adaptation paradigm, Brain Topogr. 31 (6) (2018) 1001–1013.
[106] Jaeger S. The Golden Ratio in Machine Learning. 50th IEEE Applied Imagery Pattern Recognition Workshop (AIPR), October 2021.
[107] S. Abdulhameed, T.A. Rashid, Child drawing development optimization algorithm based on child's cognitive development, Arabian J. Sci. Eng. 47 (2) (2022) 1337–1351.
[108] Y. Liu, D.J.T. Sumpter, Is the golden ratio a universal constant for self-replication? PLoS One 13 (7) (2018) e0200601.
[109] B. Pletzer, H. Kerschbaum, W. Klimesch, When frequencies never synchronize: the golden mean and the resting EEG, Brain Res. 1335 (2010) 91–102.
[110] H. Weiss, V. Weiss, The golden mean as clock cycle of brain waves, Chaos, Solit. Fractals 18 (4) (2003) 643–652.
[111] A.C. Sparavigna, M.M. Baldi, Symmetry and the golden ratio in the analysis of a regular pentagon, Int. J. Math. Educ. Sci. Technol. 48 (2) (2017) 306–316.
[112] T. Okabe, Biophysical optimality of the golden angle in phyllotaxis, Sci. Rep. 5 (2015) 15358.
[113] V.A. da Silva, et al., Two thyroid stimulating hormone assays correlated in clinical practice show disagreement in subclinical hypothyroidism patients, Clin. Biochem. 53 (2018) 13–18.

[114] W.G. Landis, P.M. Chapman, Well past time to stop using NOELs and LOELs, Integr Environ Assess Manag 7 (4) (2011) vi-viii.
[115] R.W. Flynn, et al., Serum thyroid-stimulating hormone concentration and morbidity from cardiovascular disease and fractures in patients on long-term thyroxine therapy, J. Clin. Endocrinol. Metab. 95 (1) (2010) 186–193.
[116] E. Paulsen, L.P. Christensen, K.E. Andersen, Dermatitis from common ivy (Hedera helix L. subsp. helix) in Europe: past, present, and future, Contact Dermatitis 62 (4) (2010) 201–209.
[117] A. Rasmussen, S.E. Jacob, Dandelion: an important allergen in atopic children, Dermatitis 28 (2) (2017) 166.
[118] R.K. Wagner, et al., The prevalence of dyslexia: a new approach to its estimation, J. Learn. Disabil. 53 (5) (2020) 354–365.
[119] WHO methods and data sources for global burden of disease estimates 2000-2019 Department of Data and Analytics Division of Data, Analytics and Delivery for Impact WHO, Geneva, 2020. Global Health Estimates Technical Paper WHO/ DDI/DNA/GHE/2020.3.
[120] H.T. Nguyen, et al., Why two sigma? A theoretical justification, Departmental Technical Reports (CS) 486 (2000) 10–22, https://doi.org/10.1007/978-3-540-36216-6_2.
[121] D. De Zwart, L. Posthuma, Complex mixture toxicity for single and multiple species: proposed methodologies, Environ. Toxicol. Chem. 24 (10) (2005) 2665–2676.
[122] L. Posthuma, et al., Species sensitivity distributions for use in environmental protection,assessment, and management of aquatic ecosystems for 12 386 chemicals, Environ. Toxicol. Chem. 38 (2019) 905–917.
[123] Busch, Project Report: Review on Chemical Mixture Risk Assessment Based on Chemical Monitoring – State of Knowledge and Way Forward WP 6.4.1.2. Partnership for the Assessment of Risks from Chemicals (PARC) Horizon-HLTH-2021-ENVLTH-03 CONTRACT N. 101057014, 2021.
[124] L. Yang, et al., A universal delayed difference model fitting dose-response curves, Dose Response 19 (4) (2021) 15593258211062785.
[125] S.P. Klykov, S-shaped growth curves in fermentations and golden ratio, Int. J. Biomath. (IJB) 13 (3) (2020).
[126] Chou, T.C., Drug combination studies and their synergy quantification using the Chou-Talalay method. Cancer Res. 70(2) p. 440-446.
[127] A. Hanano, et al., Differential tissue accumulation of 2,3,7,8-Tetrachlorinated dibenzo-p-dioxin in Arabidopsis thaliana affects plant chronology, lipid metabolism and seed yield, BMC Plant Biol. 15 (2015) 193.
[128] M.A. Tawfik, et al., Association between thyroid function and lipid profile parameters among obese children and adolescents, Menoufia Medical Journal 34 (3) (2021) 984–990.
[129] S. Saxena, et al., Correlation of serum thyroid stimulating hormone and prolactin in female infertility – a case control study, Indian J. Obstet. Gynecol. Res. 3 (4) (2016) 388–392.
[130] S.H. Son, et al., Consideration of serum thyrotropin when interpreting serum thyroglobulin level in patients with differentiated thyroid cancer, Int J Thyroidol 1 (2017) 5–13.
[131] Y. Liu, et al., Subclinical hypothyroidism contributes to poor glycemic control in patients with type 2 diabetes mellitus, and ellagic acid attenuates methimazole-induced abnormal glucose metabolism in mice model, J. Food Biochem. 45 (6) (2021) e13753.
[132] S. Thareja, et al., Protein tyrosine phosphatase 1B inhibitors: a molecular level legitimate approach for the management of diabetes mellitus, Med. Res. Rev. 32 (3) (2012) 459–517.
[133] S. Reza, et al., Expression of osteopontin in patients with thyroid dysfunction, PLoS One 8 (2) (2013) e56533.
[134] L. Yang, et al., Low normal TSH levels and thyroid autoimmunity are associated with an increased risk of osteoporosis in euthyroid postmenopausal women, Endocr., Metab. Immune Disord.: Drug Targets 21 (5) (2021) 859–865.
[135] G. Xanthou, et al., Osteopontin has a crucial role in allergic airway disease through regulation of dendritic cell subsets, Nat Med 13 (5) (2007) 570–578.
[136] X.C. Giner, et al., Selective ligand activity at Nur/retinoid X receptor complexes revealed by dimer-specific bioluminescence resonance energy transfer-based sensors, FASEB J 29 (10) (2015) 4256–4267.
[137] J.L. Taylor, et al., Characterization of a molecular switch system that regulates gene expression in mammalian cells through a small molecule, BMC Biotechnol. 10 (2010) 15.
[138] F. Grun, et al., Endocrine-disrupting organotin compounds are potent inducers of adipogenesis in vertebrates, Mol. Endocrinol. 20 (9) (2006) 2141–2155.
[139] L. Marinelli, et al., Docking studies on alphavbeta3 integrin ligands: pharmacophore refinement and implications for drug design, J. Med. Chem. 46 (21) (2003) 4393–4404.
[140] J. Raborn, et al., Variation in one residue associated with the metal ion-dependent adhesion site regulates alphaIIbbeta3 integrin ligand binding affinity, PLoS One 8 (10) (2013) e76793.
[141] G. Clark, et al., Integrated approach for evaluating species and interindividual differences in responsiveness to dioxins and structural analogs, Environ. Health Perspect. 98 (1992) 125–132.
[142] A. Riu, et al., Characterization of novel ligands of ERalpha, Erbeta, and PPARgamma: the case of halogenated bisphenol A and their conjugated metabolites, Toxicol. Sci. 122 (2) (2011) 372–382.
[143] J. Zhang, et al., In silico approach to identify potential thyroid hormone disruptors among currently known dust contaminants and their mMetabolites, Environ. Sci. Technol. 49 (16) (2015) 10099–10107.
[144] R.E. Frye, et al., Thyroid dysfunction in children with autism spectrum disorder is associated with folate receptor alpha autoimmune disorder, J. Neuroendocrinol. 29 (3) (2017).
[145] E.B. Gold, et al., Thyroid hormones and thyroid disease in relation to perchlorate dose and residence near a superfund site, J. Expo. Sci. Environ. Epidemiol. 23 (4) (2013) 399–408.
[146] H. Chen, et al., Perchlorate exposure and thyroid function in ammonium perchlorate workers in Yicheng, China, Int J Environ Res Public Health 11 (5) (2014) 4926–4938.
[147] A. Javidi, et al., The relationship between perchlorate in drinking water and cord blood thyroid hormones: first experience from Iran, Int. J. Prev. Med. 6 (2015) 17.
[148] D. Vesterholm Jensen, et al., No association between exposure to perfluorinated compounds and congenital cryptorchidism: a nested case-control study among 215 boys from Denmark and Finland, Reproduction 147 (4) (2014) 411–417.
[149] A.P.R. Saber, et al., The effect of ambient temperature on thyroid hormones concentration and histopathological changes of thyroid gland in cattle in Tabriz, Iran, Asian J. Anim. Vet. Adv. 4 (1) (2009) 28–33.
[150] D. Wang, et al., Data mining: seasonal and temperature fluctuations in thyroid-stimulating hormone, Clin. Biochem. 60 (2018) 59–63.
[151] Z. Kovanicova, et al., Cold exposure distinctively modulates parathyroid and thyroid hormones in cold-acclimatized and non-acclimatized humans, Endocrinology 161 (7) (2020) bqaa051.
[152] S.H. Moon, et al., Relationship between thyroid stimulating hormone and night shift work, Ann Occup Environ Med 28 (2016) 53.
[153] J.A. Kellum, Determinants of blood pH in health and disease, Crit. Care 4 (1) (2000) 6–14.
[154] L.A. Frassetto, R.C. Morris Jr., A. Sebastian, Effect of age on blood acid-base composition in adult humans: role of age-related renal functional decline, Am. J. Physiol. 271 (6 Pt 2) (1996) F1114–F1122.
[155] P. Rudas, et al., Correlation between thyroid hormone level and blood pH in cows and in their offspring, Acta Vet. Hung. 38 (1–2) (1990) 87–93.
[156] C.J. Bates, et al., Blood indices of selenium and mercury, and their correlations with fish intake, in young people living in Britain, Br. J. Nutr. 96 (3) (2006) 523–531.
[157] M. Soares de Campos, et al., Correlation between mercury and selenium concentrations in Indian hair from Rondônia State, Amazon region, Brazil, Sci. Total Environ. 287 (1–2) (2002) 155–161.
[158] M.J. Feigenbaum, Quantitative universality for a class of nonlinear transformations, J. Stat. Phys. 19 (1978) 25–52.
[159] I. Otero-Muras, P. Yordanov, J. Stelling, A method for inverse bifurcation of biochemical switches: inferring parameters from dose response curves, BMC Syst. Biol. 8 (2014) 114.
[160] G. Linage, et al., Fibonacci order in the period-doubling cascade to chaos, Phys. Lett. 359 (6) (2006) 638–639.

[161] S.H. Jarvis, Golden ratio axioms of time and space, viXra.org (2018), https://doi.org/10.13140/RG.2.2.30099.12327/5.
[162] K. Irwin, et al., Quantum walk on a spin network and the golden ratio as the fundamental constant of nature. https://quantumgravityresearch.org/portfolio/quantum-walk-on-a-spin-network-and-the-golden-ratio-as-the-fundamental-constant-of-nature/, 2017.
[163] M.W. Ho, M. el Naschie, G. Vitiello, Is spacetime fractal and quantum coherent in the golden mean? Glob. J. Sci. Front. Res. (GJSFR) 15 (1) (2015) 430–466.
[164] M.A. Verner, et al., A physiologically based pharmacokinetic model for the assessment of infant exposure to persistent organic pollutants in epidemiologic studies, Environ. Health Perspect. 117 (3) (2009) 481–487.
[165] C. Emond, et al., An assessment of dioxin exposure across gestation and lactation using a PBPK model and new data from Seveso, Environ. Int. 92–93 (2016) 23–32.
[166] A. Demond, et al., Human exposure from dioxins in soil, Environ. Sci. Technol. 46 (3) (2012) 1296–1302.
[167] M.F. Tevy, et al., Aging signaling pathways and circadian clock-dependent metabolic derangements, Trends Endocrinol. Metabol. 24 (5) (2013) 229–237.
[168] K.C. Makris, Desynchronized circadian clock and exposures to xenobiotics are associated with differentiated disease phenotypes: the interface of desynchronized circadian clock and exposures to xenobiotics would lead to adverse response and recovery, Bioessays 43 (11) (2021) e2100159.
[169] G. Rey, A.B. Reddy, Interplay between cellular redox oscillations and circadian clocks, Diabetes Obes. Metabol. 17 (2015) 55–64.
[170] K. Ikegami, et al., Interconnection between circadian clocks and thyroid function, Nat. Rev. Endocrinol. 15 (10) (2019) 590–600.